Correcting the Stress-Strain Curve in Hot Compression Process to High Strain Level

Y.P. LI, E. ONODERA, H. MATSUMOTO, and A. CHIBA

This article provides a model that regards the evolution behavior of the friction coefficient in the cylindrical compression test as a function of true strain on the basis of experimental results, allowing the effect of friction on the deformation curve at extremely high strain level to be evaluated and corrected for the first time. The compressive tests were carried out at a stroke rate of 1.2 mm/s on IHS38MSV hypoeutectoid steel with various lubricants at temperatures ranging from 800 °C to 1200 °C. The results showed that the friction coefficient for the compressive process was not constant and the variation could be approximated by an exponential equation along with the true strain. Microstructure observation showed that the stress increase in the later stages of process should be closely related to the large increase in the friction coefficient. The corrected curves were found to correlate well with the microstructure observation.

DOI: 10.1007/s11661-009-9783-7

I. INTRODUCTION

BULK deformation processes that involve large strains and a high strain rate such as rolling, forging, and extrusion are usually conducted at temperatures higher than approximately two-thirds the melting point of the material. A fundamental method in investigating the working behavior of materials is analyzing the true stress–true strain curves combined with the microstructure observation, which reflects their intrinsic mechanical properties of materials. However, friction between the material and the tools during the working process have to be considered before further investigation,[1–5] because practical measurements of the deformation curve depart from the real mechanical response of the materials to a certain degree. In practice, for many metalworking processes friction is the predominant factor. The friction between a working piece and the jig can lead to heat generation, wear, pickup and galling of the tool surface, which contributes to the premature failure of the tools.[3–5] Friction increases nonhomogeneous deformation, leading to defects in the finished products. In addition, friction affects the evaluation of the deformation behavior of materials because the flow stress of the sample is strongly influenced by friction; this is especially true in hot compression processes,[6] where the friction is hard to eliminate completely even when the lubricant is added between the sample and anvil surfaces.[7] Therefore, reducing the friction coefficient during the metalworking process and correcting the deformation curve for real behavior are very important topics for both researchers and engineers in hot working.

Y.P. LI, Researcher, E. ONODERA, Researcher, H. MATSUMOTO, Assistant Professor, and A. CHIBA, Professor, are with the Institute of Materials Research, Tohoku University, Sendai, Japan. Contact e-mail: a.chiba@imr.tohoku.ac.jp
Manuscript submitted May 22, 2008.
Article published online February 10, 2009

Usually, lubricants are added to reduce the friction coefficient. However, this is not always effective especially in large strain deformation process, because the lubricants are only effective up to a limited strain level. At higher strain levels such as those for the cylindrical hot compression process shown in Figure 1, the lateral side of the sample without lubricant came closer to the anvil surface in compression as the strain level increased due to barreling, and it subsequently came into contact with the anvil surface. This lateral side later formed the outer area of the contacting surface when the strain attained a certain level, leading to sticking in the outer area of the sample or a great increase in the friction coefficient based upon some preliminary observations. In practice, directly predicting the friction coefficient at a random strain level is difficult because of the difficulty in measuring related parameters of specimens in the working process; researchers often simply assume that the friction coefficient is a constant or independent of the strain level.[5,8–11] The details about the evolution behavior of friction coefficients in working processes have not yet been made clear. In this case, the stress-strain curve can only be effectively plotted for a limited strain level (lower than 0.6 or 0.7),[8–11] because at higher strain levels a great increase in the applied stress occurs due to an abnormal increase in the friction coefficient; this cannot be corrected properly by the assumed average friction coefficient.[8,11–13] Therefore, in order to correct the deformation curves in large strain compression processes a basic evolutional model of the friction coefficient as a function of strain needs to be proposed.

In previous research,[11,14–17] some methods evaluating the average friction coefficient in bulk metal forming were proposed for cylindrical specimens and were shown to be effective to a certain degree when the sample was deformed with a relatively lower strain level; a typical formulation was given by[11,14]

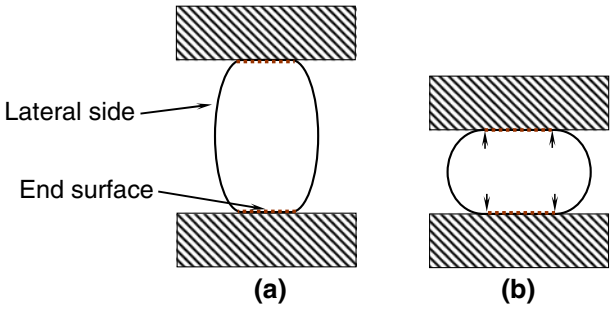

Fig. 1—Schematic figures of the specimen shape change during compression process (*a*) at lower strain level and (*b*) at higher strain level.

$$\mu = \frac{\frac{R}{h} \cdot b}{\frac{4}{\sqrt{3}} - \frac{2b}{3\sqrt{3}}} \quad [1]$$

where μ is the average friction coefficient of the entire working process varying from 0 (perfect sliding) to 1 (sticking), b is the barreling factor, and R and h are the theoretical radius and final height of the sample respectively; b is given by[11,14]

$$b = 4\frac{\Delta R}{R} \cdot \frac{h}{\Delta h} \quad [2]$$

where ΔR and Δh are the differences between the maximum radius R_m and the top radius R_t of the sample and the reduction in height for the cylinder after compression, respectively. In this article, based upon Eq. [1] the instantaneous friction coefficient μ_s is evaluated quantitatively as a function of the strain level. Therefore, correcting the deformation curve to extremely high strain levels should be possible.

The IHS38MSV hypoeutectoid steel with a carbon content of approximately 0.41 pct was chosen for this study. Hypoeutectoid steel is widely used in industrial applications due to its superior mechanical properties. By basing the evolution behavior of the instantaneous friction coefficient as a function of strain as a model, a precise method in correcting the deformation curves to high strain level is developed here for the first time. The sample has a cylindrical shape similar to that of Ebrahimi *et al.*[11,14] as this simplifies the evaluation and computation of the friction coefficient.

II. EXPERIMENTAL PROCEDURES

The IHS38MSV hypoeutectoid steel (Sumitomo Metal Industries, Ltd., Osaka, Japan) was selected for the current study. Details about the composition of the materials are described in Table I. Cylindrical specimens, 8 mm in diameter and 12 mm in height, were formed by electrodischarge machining from the outer section of a huge forged cylinder. The flat ends of the specimen were machined with spiral grooves with depths of 0.1 mm so that at high temperatures the lubricant, which is in a molten state, can flow freely inside of the grooves. A preliminary examination by optical microscope of the sample along its lateral side showed that the microstructure was mainly composed of bright ferrites and dark pearlites not uniformly distributed with grain sizes ranging from 10 to 50 μm, as shown in Figure 2.

Table I. Chemical Composition of the Hypoeutectoid Steel IHS38MSV

Element	C	Si	Mn	P	S
Weight percent	0.41	0.56	1.17	0.20	0.47

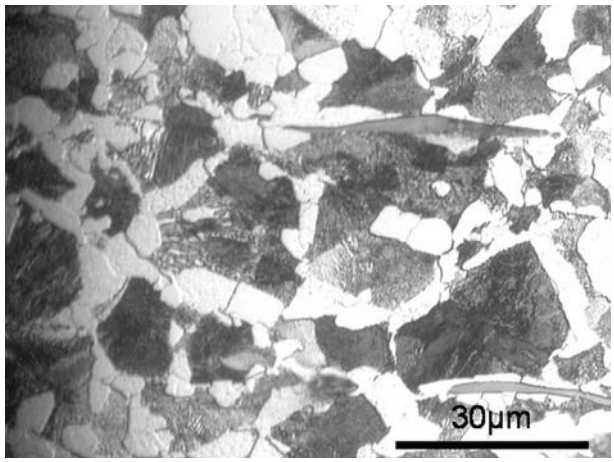

Fig. 2—Microstructure of the undeformed IHS38MSV hypoeutectoid steel.

Compression tests were carried out in vacuum at 800 °C, 900 °C, 1000 °C, 1100 °C, and 1200 °C, respectively, using a computer-aided Thermecaster-Z (Fuji Denpa Kogyo Co. Ltd., Osaka, Japan) hot forging simulator. The chosen stroke rate was 1.2 mm/s. A heating rate of 5 °C/s from room temperature to the scheduled temperatures was carried out by induction. The sample was maintained at an elevated temperature for 300 seconds before compression. As soon as the sample was compressed to the final strain level, a mixture of N_2 (6 MPa pressure) and He (4 MPa) was used to quench the sample to room temperature at a cooling rate of approximately 50 °C/s. The thermocouple used is R-type, and the temperature accuracy was approximately ± 3 °C according to the parameters cited in the equipment guidebook. There were four kinds of lubricants used, and the lubricant with the lowest average friction coefficient in compression was to be chosen for further investigation. The details for the lubricants are shown in Table II.

In order to evaluate the friction coefficient evolution behavior as a function of strain level, the samples were compressed to strain levels of about 0.2, 0.4, 0.6, 0.8, 1.0, 1.2, 1.4, and 1.6, respectively. The friction coefficients before each strain level were calculated using Eq. [1]. It should be noted that the friction coefficient μ calculated by Eq. [1] is the mean value from 0 to the measured strain level; the instantaneous friction coefficient μ_s at a specific strain level has to be estimated later. By using the instantaneous friction coefficient estimations at specific strain levels, a model showing the

Table II. Information about the Lubricants Used in Present Study

Number	Name	Chemical Component	Producer	Melting Point
1	Moly paste 500 spray	MoS_2	Sumitomo Lubricant Co., Ltd., Japan	—
2	Deltaglaze 347HS	Isopropyl Alcohol	Acheson Japan Limited, Kakogawa, Japan	900 °C to 1050 °C
3	Deltglaze 349	Acetic acid *n*-butyl	Acheson Japan Limited	850 °C to 950 °C
4	Mixture	1 + 2 + 3	—	—

evolution behavior of instantaneous friction coefficient as a function of true strain can be proposed.

The microstructure observation was conducted by optical microscope. The samples were machined gradually by different grades of sandpapers and finally polished with a solution containing SiC particles with a mean diameter of 0.03 μm. The etching was carried out in a 4 pct HNO_3 solution of alcohol before observation.

III. RESULTS AND DISCUSSION

Figure 3 shows the true stress–true strain curves at 1000 °C when using various lubricants. The deformation curves with the lubricants clearly show relatively lower stresses compared to the one without the lubricant in all cases. In the deformation processes with the lubricants excluding the mixture, the deformation curves were all shown to be approximately at the same level when the strain was lower than 0.6. However, the true stress–true strain curve when using a mixture of the three lubricants showed much lower stress over the entire stage. Abnormal increases in the stress were observed at large strain levels for all cases. The experiment was carried out with a stroke rate controlling process: a gradual increase of strain rate proportional to the inverse of the sample height. However, for the instance shown in Figure 3, the experimental was conducted with the same conditions except for the difference in the lubricant. The effect of strain rate sensitivity on the stress is thought to be same. Therefore, the difference between the stress levels especially at large strain levels can reasonably be ascribed to the lubricating effect.

The average friction coefficients of different lubricants calculated using Eq. [1] are shown in Figure 4. It was observed that the sample lubricated with mixed lubricants showed the lowest friction coefficient of about 0.65. Similar deformation behaviors were also observed at 800 °C, 900 °C, 1100 °C, and 1200 °C. At 800 °C, the Moly paste 500 spray (MoS_2) showed the lowest friction coefficient. From 900 °C to 1200 °C, a mixture of Moly paste 500 spray, Deltaglaze347HS, and Deltaglaze349 with a volume ratio of approximately 1:1:1 showed the best results. From the results, Moly paste 500 spray seemed to be suitable at a relatively low-temperature forging process for the materials, possibly due to its excellent resistance to sticking between the jig and sample surfaces.[18] However, MoS_2 is unstable and easily decomposes into Mo and S at high temperature. Above 900 °C, additions of Deltaglaze347HS and Deltaglaze349 seemed helpful to improving the lubricating effect of MoS_2, which may have been due to their protection of MoS_2 through dilution or chemical catalysis from decomposition, as well as their excellent lubricating effects above 900 °C.[19]

The true stress–true strain curves at various temperatures using the appropriate lubricant with the lowest average friction coefficient as mentioned previously were plotted in Figure 5. An expected decrease in flow stress was observed when the testing temperature was increased. In addition, a common phenomenon was an increase in the applied stress due to the great increase in friction coefficient when the strain was higher than 0.6,

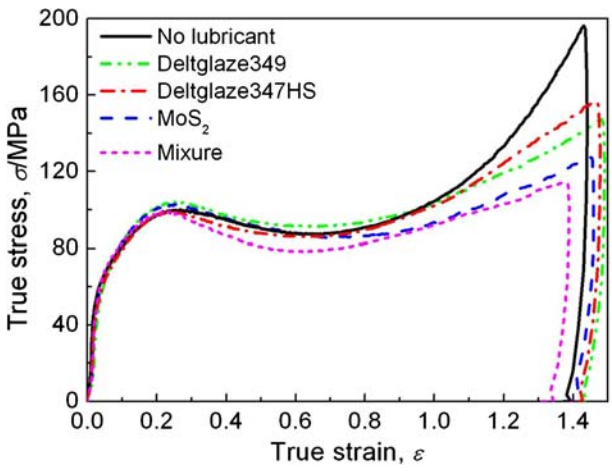

Fig. 3—True stress–true strain curves for samples with different lubricants at 1000 °C.

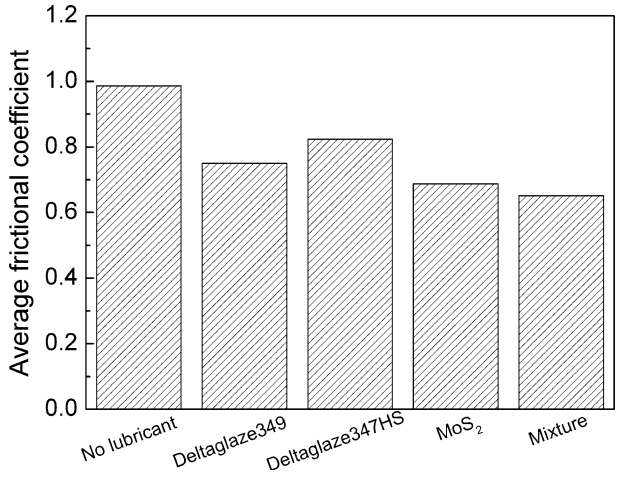

Fig. 4—Average friction coefficient of compression process with different lubricants when compressed to strain of about 1.6 at 1000 °C.

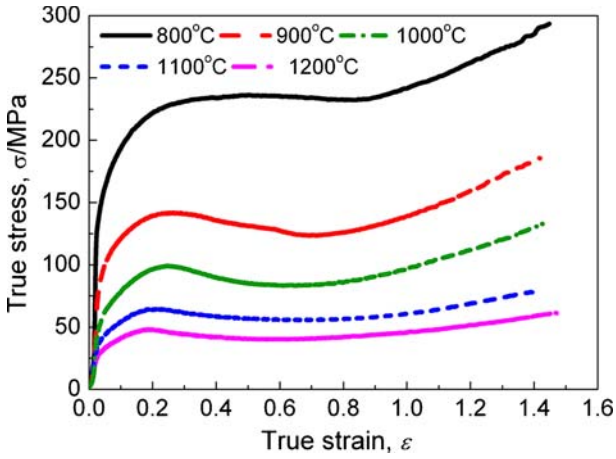

Fig. 5—True stress–true strain curves obtained at different temperatures.

although the effect of strain rate sensitivity was not negligible for this instance. Detailed research regarding the correction from the stroke rate controlling process into the strain rate-controlling process was conducted in subsequent research by the current authors.[20] The portion of stress increase due to friction has to be corrected for further use. In order to correct the stress at high strain levels, the friction coefficient as a function of strain has to be investigated further in detail.

The profiles of the sample surfaces when compressed to a list of strain levels at 1000 °C are shown in Figure 6(a). This lubricant was the mixture of the three others. The sample surfaces at other temperatures also showed similar profiles to that of 1000 °C. At strains lower than about 0.5, the top surface profiles of the samples after compression were formed mainly by the end surfaces of the samples with grooves; in this instance the top radius R_T was approximately equal to the radius of the contacting surface of the deformed sample with anvil. However, at higher strain levels (strain higher than approximately 0.6), the contacting profiles were observed to be formed by both the top surface (characterized by the groove profiles in the Figure 6(b)) in the middle area and the area formed from the side surface of the sample without groove in the outer area. In this instance, R_T was determined by the profiles of the grooves, as demonstrated in Figure 6(b).

The average friction coefficients at different strain levels were determined with either Eq. [1][14] or

$$\mu = \frac{3\sqrt{3}R\Delta R}{3\Delta HR - 2\Delta RH} \text{ or } = \frac{3\sqrt{3}}{3\frac{\Delta H}{\Delta R} - 2\frac{H}{R}} \qquad [3]$$

Equation [3] is a simplification of Eq. [1] derived by inserting Eq. [2] into Eq. [1]; calculating the average friction coefficient with Eq. [3] is more convenient than that with Eq. [1] since the barreling factor is not calculated directly in this situation. Equations [1] and [3] were obtained based upon an upper-bound theorem of rigid perfectly plastic materials.[14] The average friction coefficients at different temperatures were plotted in Figure 7 as a function of true strain. The average friction coefficient was observed to increase with the increasing strain level. These results did not conform to the conventional viewpoint[8,14] that the friction coefficient as a function of strain level is a constant. There are several reasons existing for the increase in the friction coefficient with an increasing strain level. First, the end surface area of the sample broadens accordingly, causing the lubricating effectiveness to worsen as it decreases the thickness of the lubricant film. In addition, the lateral side of the sample without the lubricant comes closer to the compression jig surface with increasing strain levels and comes into contact with the jig surface, forming the outer area of the contacting surface shown in Figure 6(b) when the strain reached a certain level (0.6 to 0.8). In this instance, the friction coefficient increases abnormally, causing the stress to increase greatly. In the compression process, an increase in strain level causes the condition of the sample surface to vary gradually, which causes a corresponding increase in the friction coefficient. In this study, the parameters in Eq. [3] were measured three to four times along various directions of the deformed samples; the mean values of the measured results were then used.

If it is supposed that μ_n and μ_{n-1} are the average friction coefficients when samples are directly compressed to the two neighboring strains of ε_n and ε_{n-1}, the instantaneous friction coefficient μ_s at a strain level of $(\varepsilon_{n-1} + \varepsilon_n)/2$ can be given from the integral mean value exploration of this small strain range by

$$\mu_{s(\varepsilon_{n-1}+\varepsilon_n)/2} = \frac{\int_0^{\varepsilon_n} \mu_n d\varepsilon - \int_0^{\varepsilon_{n-1}} \mu_{n-1} d\varepsilon}{\varepsilon_n - \varepsilon_{n-1}} = \frac{\varepsilon_n \mu_n - \varepsilon_{n-1}\mu_{\varepsilon_{n-1}}}{\varepsilon_n - \varepsilon_{n-1}} \qquad [4]$$

where it was supposed that the instantaneous friction coefficient followed linear behavior. Thus, the average friction coefficient of this short strain range was found to be equal to the instantaneous friction coefficient $\mu_{s(\varepsilon_{n-1}+\varepsilon_n)/2}$ at the strain $(\varepsilon_{n-1} + \varepsilon_n)/2$.

The instantaneous friction coefficients μ_s for the testing temperatures 800 °C to 1200 °C and calculated with Eq. [4] are plotted in Figures 8(a) through (e) as a function of strain. The instantaneous friction coefficient μ_s was relatively lower at lower strain levels and increased rapidly when the strain was higher than 0.6 compared to the corresponding average friction coefficient, as shown in Figure 7. The values of the initial friction coefficients varied in a range of 0.2 to 0.3, showing very slight effects of friction or well lubricating effectiveness in the initial stages of the compression process. In addition, the instantaneous friction coefficient μ_s did not vary in large ranges when the strain was lower than 0.6 at nearly all temperatures. This may be why previous researchers considered the friction coefficient to be a constant when the strain level was relatively low.[9,11–15] At higher strain levels, the instantaneous friction coefficient increased rapidly as the strain increased. At strains of 1.4 to 1.5, there seemed to be a decrease in some values of the instantaneous friction coefficients. This was thought to be mistaken considering the change of the sample shape after deformation

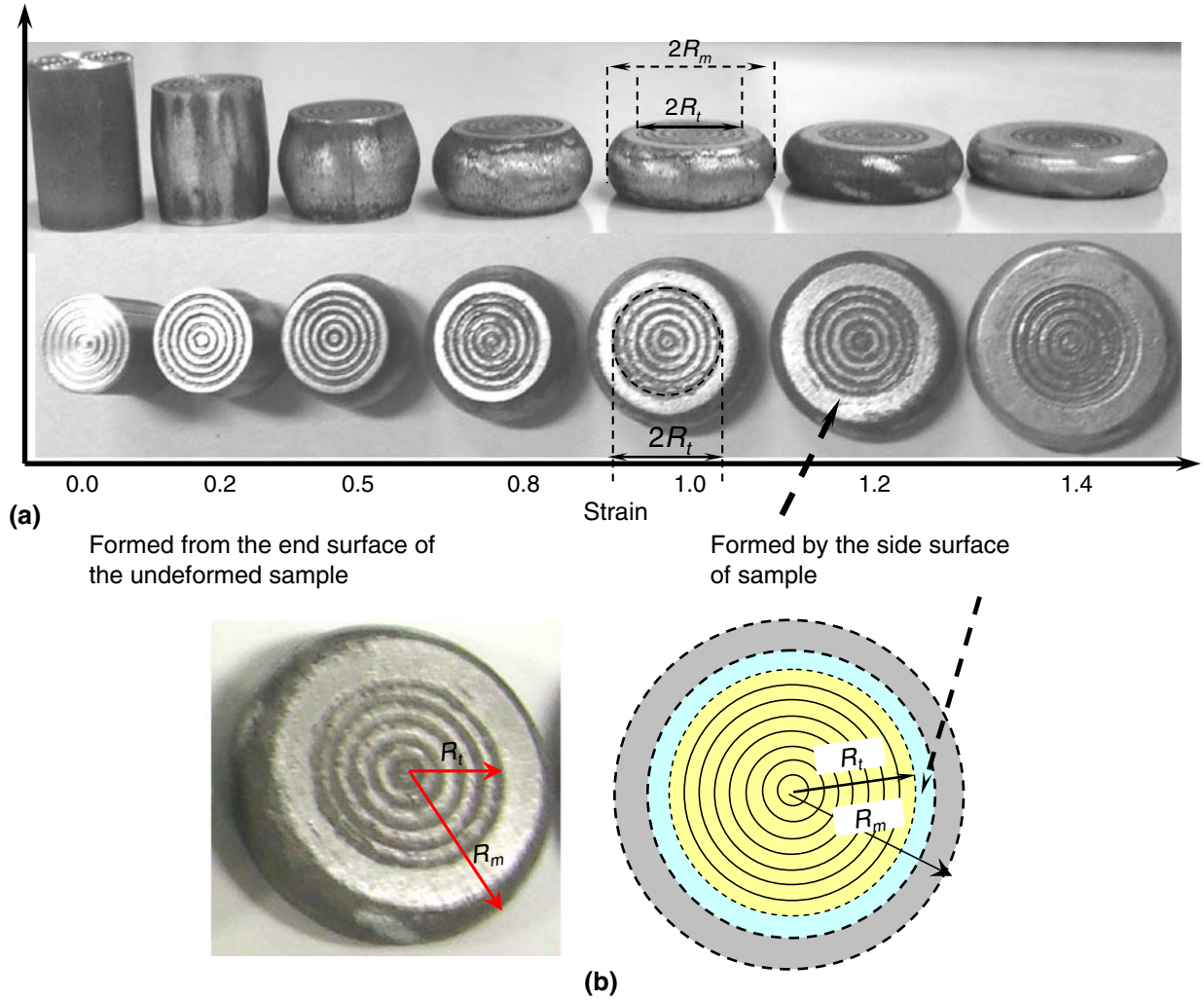

Fig. 6—(*a*) Photos of the sample when compressed to different strain levels at 1000 °C. (*b*) Amplified profile and the corresponding schematic figures of the contacting surface of the deformed samples at large strain level.

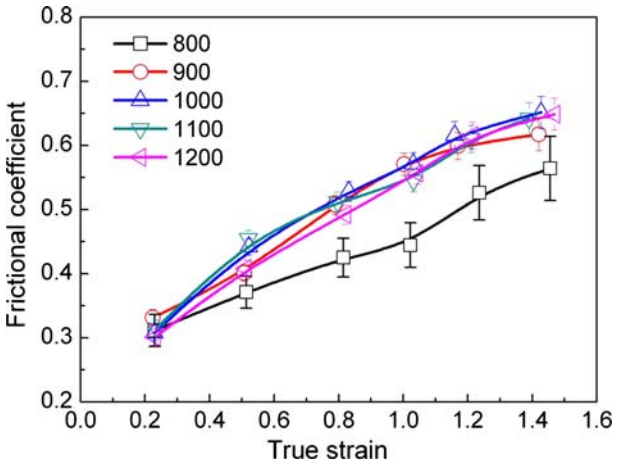

Fig. 7—Average friction coefficients of samples when compressed to different strain levels.

and the described analysis. When calculating the friction coefficient, the profiles of the grooves after deformation could easily be recognized at lower strain levels. However, at higher strain levels, the boundary between groove profiles and the area formed by the lateral side of the sample became blurry and difficult to determine due to the flattening of the grooves, which may have led to large errors in calculating the instantaneous friction coefficient, as shown in Figure 8. In addition, a small variance of value in the top radius of the deformed sample had a great effect on the calculated results using Eq. [3]. Therefore, the data at high strain levels showed large variances compared to lower strain levels. By employing the changing behavior of the obtained data, a suitable empirical function was found using an exponential fitting process

$$\mu_s = \mu_0 + A \exp(\varepsilon/\varepsilon_0) \qquad [5]$$

where μ_0, A, and ε_0 are constants that are all necessarily larger than zero and the best fit values are of these parameters are summarized in Table III. Even though Eq. [5] was obtained for the specific hot-forging process of the present steel, this equation is also applicable to other high strain levels hot-forging process of metallic materials since the friction coefficient is related to

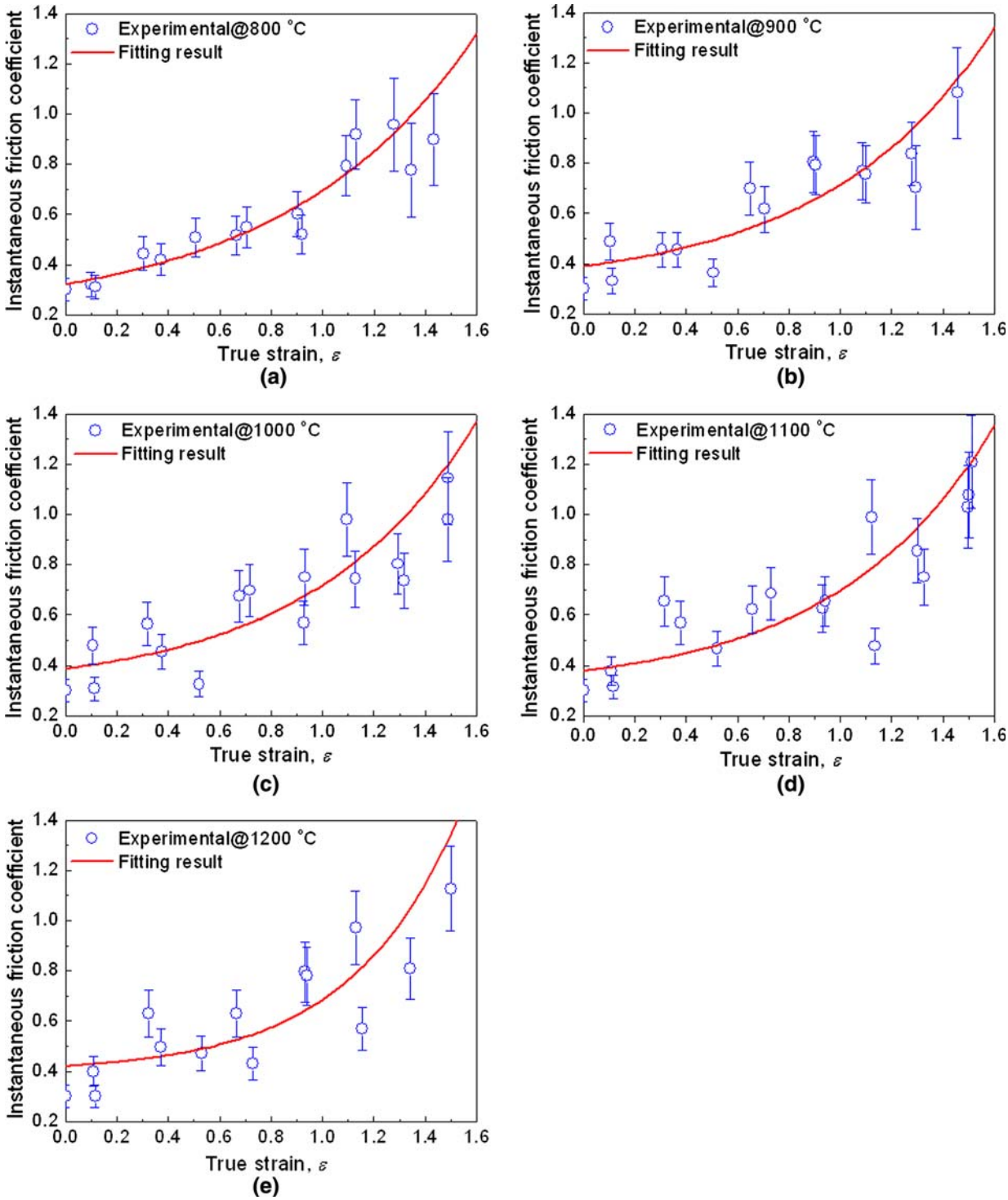

Fig. 8—Instantaneous friction coefficient at different strain levels and the fitting results at (*a*) 800 °C, (*b*) 900 °C, (*c*) 1000 °C, (*d*) 1100 °C, and (*e*) 1200 °C.

general characteristics of the forging process, such as the barreling of sample and variation in effects of lubrication on deformation.

Using DEFORM-3D v6.130 software,[21] the shapes of the samples in the hot-forging process were simulated by using Eq. [5] at 1000 °C. The typical sample profiles at strain levels of 0.3 and 0.65 are demonstrated in Figures 9(a) and (b), respectively. The top surface of the compressed sample was formed mainly from its original top surface at lower strain level (lower than 0.6), while at higher strain levels (higher than 0.6) the outer area of the contacting surface is from the side surface due to the gradually increased friction coefficient; this correlates with the current experimental results very well. The top

Table III. Parameters Used in Fitting Processes

Temperature	μ_0	A	ε_0
800 °C	0.18811	0.13371	0.74878
900 °C	0.1083	0.25336	1.0857
1000 °C	0.3001	0.08755	0.63895
1100 °C	0.3002	0.07844	0.61564
1200 °C	0.3935	0.02739	0.42256

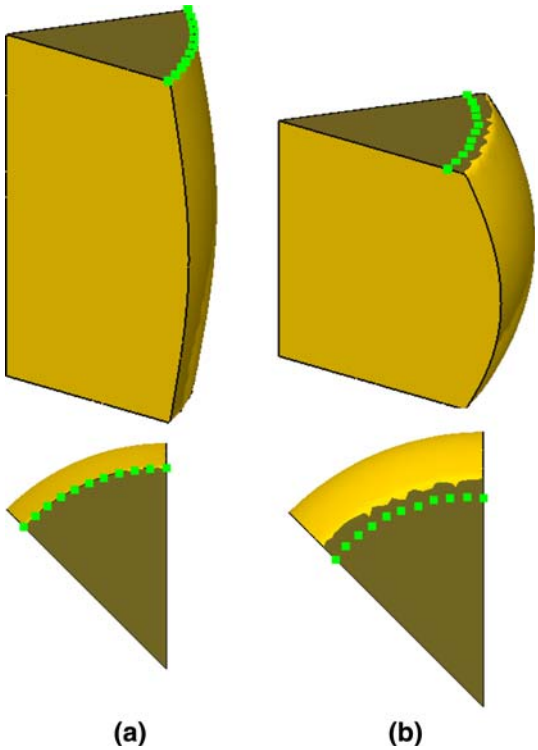

Fig. 9—Shape of the sample at strain levels of (*a*) 0.3 and (*b*) 0.65 simulated by DEFORM software at 1000 °C.

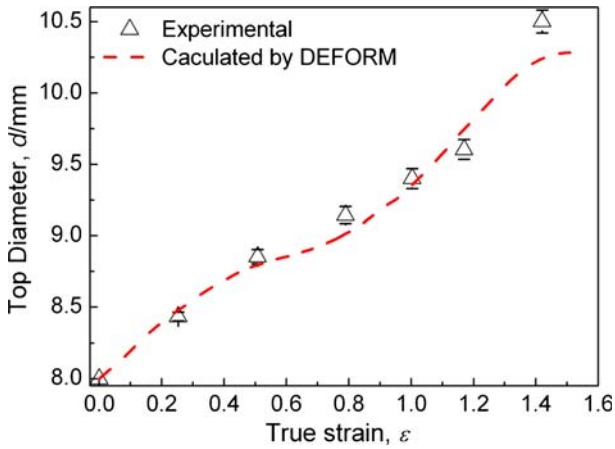

Fig. 10—Top diameter of the samples R_t at different strain levels by (*a*) experiment and (*b*) simulation at 1000 °C.

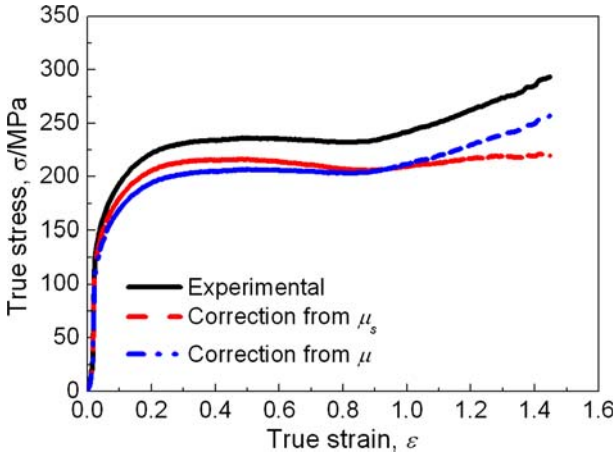

Fig. 11—Deformation curves corrected by instantaneous friction coefficient and average friction coefficient at 800 °C.

diameters R_t at different strain levels can also be derived by DEFORM simultaneously, as shown in Figure 10. There was very good agreement between the calculated and the measured results, demonstrating that the model for the instantaneous friction coefficient expressed by Eq. [5] is appropriate and suitable to large-strain hot-forging processes. It is interesting to observe that the value of the instantaneous friction coefficient was higher than 1 at higher strain levels if calculated with Eq. [5], which contradicts previous results showing that the friction coefficient is constant and lower than 1 in compression processes from Tresca's law.[12] From the simulation results in Figure 10, the top diameter of sample R_t does not expand any more when the strain level is higher than 1.4 at 1000 °C. Here, the interface between the sample and anvil is thought to evolve to a static frictional state, where the friction coefficient can be higher than 1 in many cases. This theorem, regarding the static friction coefficient and the evolution from kinetic friction into static friction in hot-forging process for large strain levels, can provide a new field of study to researchers in this field.

If the thickness of the specimen is small enough, the axial compressive stress is constant through the thickness. In this case, the friction of the deformation curve can be corrected by[8,11,14]

$$\sigma = \frac{C^2 P}{2[\exp(C) - C - 1]} \qquad [6]$$

where $C = \frac{2\mu r}{h}$, and r and h are the original radius and the height of the sample.[11,14] In previous research,[8,11,14,15] μ was a constant. In this article, μ is replaced by the instantaneous friction coefficient obtained from Eq. [5]. Therefore, by combining Eqs. [5] and [6], the correction of true stress–true strain curves for a large deformation strain can be realized for the first time.

Figure 11 shows the true stress–true strain curves at 800 °C without correction and the curves corrected by the average friction coefficient μ at strain level of 1.5 and the instantaneous friction coefficient μ_s, respectively. The difference between these two methods is

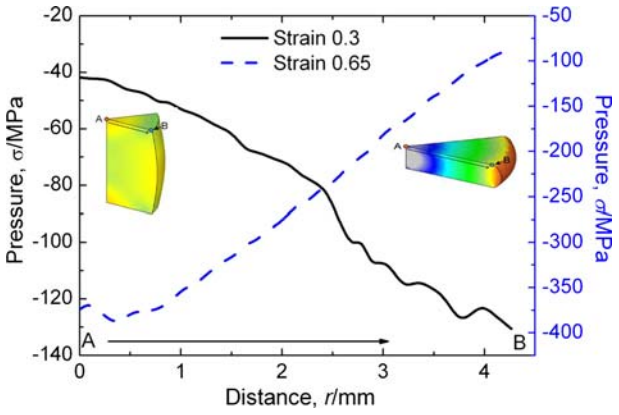

Fig.12—Pressure distributions at strains of 0.3 and 0.65 as a function of the distance from the center of sample top surface.

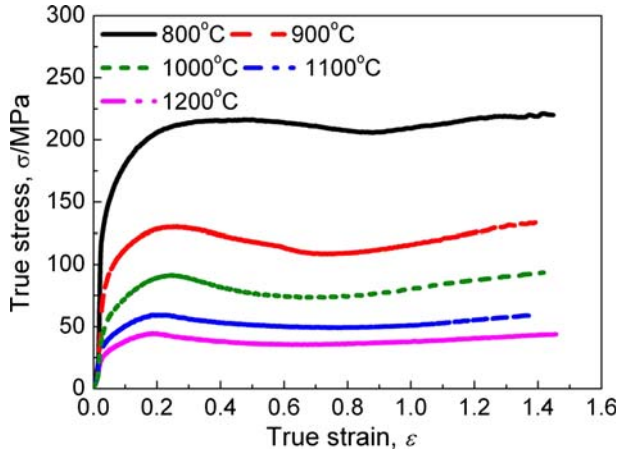

Fig. 13—True stress–true strain curve after all corrections at different temperatures.

clearly observed. The correction by the average friction coefficient μ for the entire compression process is a nearly proportional reduction of the original data, while the correction by the instantaneous friction coefficient μ_s is more practical because the variation in the friction coefficient was taken into account. It is important to note that in the correction procedure using Eq. [6], the frictional behavior fits with Coulomb's law, which states that the axial compressive stress over the diameter of the sample is symmetrical about the centerline and rises to a sharp peak at the center of the sample, which is called the friction hill.[12] However, from simulation results of pressure distribution over diameter, a great discrepancy of pressure distribution was found between the large-strain hot-forging process examined in this article and low-strain processes. The stress at lower strain levels fits with the Coulomb distribution very well, as shown in Figure 12 (strain of 0.3); however, at high strain levels, a reverse Coulomb distribution was observed in the DEFORM software calculations, probably due to sticking of the outer area of the top surface with the compression anvil (strain 0.65). However, the correction process developed in this article should be still effective; since Eq. [6] is derived from the average value of pressure across the sample surface, the overall effect applied to the sample should be approximately the same.

The stress-strain curves corrected by instantaneous friction coefficient up to a strain of 1.5 for temperatures of 800 °C to 1200 °C are plotted in Figure 13, in which other corrections due to adiabatic temperature increment, stroke-rate effects were also carried out in other research by the authors.[8,20] When compared to the experimental results in Figure 5, the stress increases at higher strain levels are all adjusted to near constants or slight increases with an increase in strain, which can be explained by the equilibrium state between the work hardening and the dynamic recrystallization processes.

The microstructure of the samples at a temperature of 1000 °C and strain levels of 0.2, 1.2, and 1.6 are shown in Figures 14(a) through (c), respectively. The deformed microstructure appears completely different compared to the original one shown in Figure 2. The bright ferrite and the dark pearlite of the original microstructure disappeared and the grain boundaries became blurred because of the formation of the martensitic phase in the rapid cooling process immediately after completion of the compression process. In this study, the hot compression process was conducted above the eutectoid line of steel (~727 °C). The phase constituent was thought to be austenite because of the long holding time (300 seconds) at 1000 °C. The process was followed by a quick cooling rate of about 50 °C/s to room temperature as soon as the compression process was finished. Thus, the grain boundaries in Figure 14 should be the austenite grain boundaries as they cannot move actively due to high cooling rate, though there were numerous fine martensitic phases inside of the original austenitic grains. The grain size of the austenite at different strain levels was more uniformly distributed compared to the original ferrite and pearlite structure. The constant grain size of the austenite phase when compressed to a strain level of 0.2 was 15 to 20 μm, while the grain size at strain levels of 1.2 and 1.6 were a little smaller at 10 to 15 μm, showing that there was a gradual decrease in grain size by dynamic recrystallization after the strain level of 0.2. In the strain range of 1.2 to 1.6, the equilibrium state of deformation between work hardening and recrystallization was thought to exist because no difference between the microstructures at these two strain levels was observed between Figures 14(b) and (c). These results, showing a steady or equilibrium state of deformation curves after correction at higher strain levels, correlated well with the observation of an equilibrium state of deformation mechanism at higher strain levels; this shows that the correction by the instantaneous friction coefficient developed in this study is appropriate.

IV. CONCLUSIONS

The thermomechanical behavior of IHS38MSV hypoeutectoid steel and the evolution behavior of the instantaneous friction coefficient as a function of strain

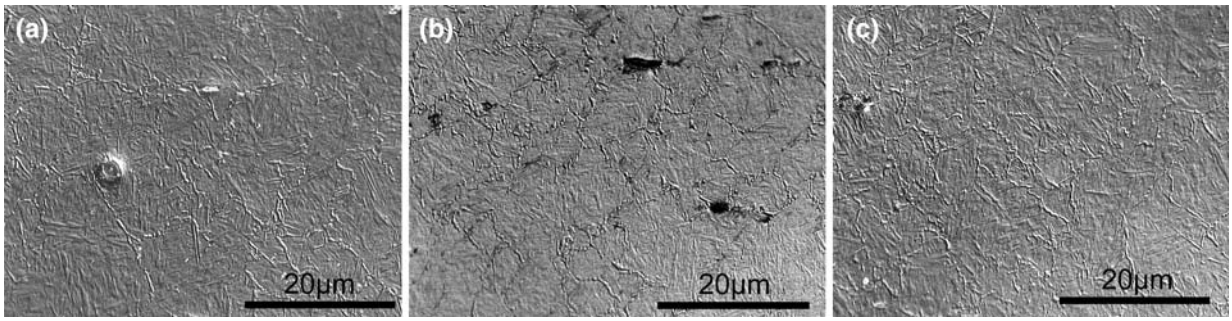

Fig. 14—Microstructures of the samples when compressed to different strain levels at 1000 °C.

were studied for hot compression process and the results obtained are as follows.

1. For the hot compression process for IHS38MSV steel, the most suitable lubricant at 800 °C was Moly paste 500 spray; a mixture of Moly paste 500 spray, Deltaglaze347HS, and Deltaglaze349 was suitable at temperatures in the range 900 °C to 1200 °C.
2. The friction coefficient was not a constant in the compression process and varied in an approximate exponential relationship with strain according to the fitting results.
3. By using the exponential relationship between the instantaneous friction coefficient μ_s and the true strain, the deformation curves could be corrected for very large strain levels and showed better results than when the average friction coefficient was used.
4. The variation of the sample shape calculated by DEFORM software using the instantaneous friction coefficient correlated well with the experimental results.

ACKNOWLEDGMENTS

This research was supported by a Cooperation of Innovative Technology and Advanced Research in Evolutional Area from Ministry of Education, Culture, Sports, Science and Technology of Japan. The authors of this research thank Yamanaka Eng. Co. Ltd., Osaka, Japan for partly supporting this research.

OPEN ACCESS

REFERENCES

1. Z. Gao and R.V. Grandhi: *Int. J. Mach. Tools Manuf.*, 2000, vol. 40, pp. 691–710.
2. H. Monajati, M. Jahazi, R. Bahrami, and S. Yue: *Mater .Sci. Eng.*, 2004, vol. A373, pp. 286–93.
3. L. Briottet, J.J. Jonas, and F. Montheillet: *Acta Mater.*, 1996, vol. 44, pp. 1665–72.
4. N. Bay: *J. Mech. Work. Technol.*, 1987, vol. 14, pp. 203–23.
5. A.T. Male and V. Depierre: *J. Lubr. Technol.*, 1970, vol. 92, pp. 389–97.
6. F.P. Bowden and D. Rabor: *The Friction Lubrication of Solid*, 1st ed., Oxford University Press, London, 1950, p. 1.
7. J.A. Schey: *Tribology in Metalworking: Friction, Lubrication and Wear*, ASM, Metals Park, OH, 1983, p. 1.
8. H. Monajati, M. Jahazi, S. Yue, and A.K. Taheri: *Metall. Mater. Trans. A*, 2005, vol. 36A, pp. 895–905.
9. G.W. Pearsall and W.A. Backofen: *Trans. ASME. Ser. D: J. Basic Eng.*, 1963, vol. 85B, pp. 68–75.
10. G.T. van Rooyen and W.A. Backofen: *Int. J. Mech. Sci.*, 1960, vol. 1, pp. 1–27.
11. R. Ebrahimi, A. Najafizadeh, and R. Shateri: *Proc. Steel Symp. 81*, Iranian Institute for Iron and Steel, Isfahan, Iran, Mar. 2–3, 2003, pp. 230–37.
12. G.E. Dieter: *Mechanical Metallurgy*, 3rd ed., McGraw Hill Book Co., New York, NY, 1986, p. 539.
13. S.I. Oh, S.L. Semiatin, and J.J. Jonas: *Metall. Trans. A*, 1992, vol. 23A, pp. 963–75.
14. R. Ebrahimi and A. Najafizadeh: *J. Mater. Process. Technol.*, 2004, vol. 52, pp. 136–43.
15. D.Y. Cai, L.Y. Xiong, W.C. Liu, G.D. Sun, and M. Yao: *Mater. Charact.*, 2007, vol. 58, pp. 941–46.
16. N. Frederiksen and T. Wanheim: *J. Mech. Work. Technol.*, 1985, vol. 12, pp. 261–68.
17. N. Bay: *J. Mech. Work. Technol.*, 1987, vol. 14, pp. 203–23.
18. http://www.sumico.co.jp.
19. http://www.achesonindustries.com.
20. Y.P. Li: *Metall. Trans. A*, 2008, vol. 39A.
21. http://www.yamanaka-eng.co.jp.